Belg. J. Zool., 142 (2) : 101-113 July 2012

A qualitative comparison of 3D visualization in *Xenopus laevis* using a traditional method and a non-destructive method

Emilie Descamps[1,*], Jan Buytaert[2], Barbara De Kegel[1], Joris Dirckx[2] & Dominique Adriaens[1]

[1] Research Group Evolutionary Morphology of Vertebrates, Ghent University, K.L. Ledeganckstraat 35, 9000 Ghent, Belgium.
[2] Laboratory of BioMedical Physics, University of Antwerp, Groenenborgerlaan 171, 2020 Antwerp, Belgium.

* Corresponding author: Emilie Descamps. E-mail: emilie.descamps@ugent.be

ABSTRACT. Many tools are currently available to investigate and visualize soft and hard tissues in animals both in high-resolution and three dimensions. The most popular and traditional method is based on destructive histological techniques. However, these techniques have some specific limitations. In order to avoid those limitations, various non-destructive approaches have surfaced in the last decades. One of those is micro-CT-scanning. In the best conditions, resolution achieved in micro-CT currently approaches that of standard histological protocols. In addition to bone, soft tissues can also be made visible through micro-CT-scanning. However, discriminating between structures of the same tissue and among different tissue types remains a challenge. An alternative approach, which has not yet been explored to its full potential for comparative anatomy studies, is Orthogonal-Plane Fluorescence Optical Sectioning (OPFOS) microscopy or tomography, also known as (Laser) Light Sheet based Fluorescence Microscopy (LSFM). In this study, we compare OPFOS with light microscopy, applying those techniques to the model organism *Xenopus laevis*. The potential of both methods for discrimination between different types of tissues, as well as different structures of the same tissue type, is tested and illustrated. Since the histological sections provided a better resolution, adjacent structures of the same tissue type could be discerned more easily compared to our OPFOS images. However, we obtained a more naturally-shaped 3D model of the musculoskeletal system of *Xenopus laevis* with OPFOS. An overview of the advantages and disadvantages of both techniques is given and their applicability for a wider scope of biological research is discussed.

KEY WORDS: vertebrates, histological sectioning, optical sectioning, *Xenopus*, 3D visualization.

INTRODUCTION

Three-dimensional (3D) visualization tools have been applied in biological sciences for decades (e.g. Afshar & Dykes, 1982; Johnson & Capowski, 1983; Vanden Berghe et al., 1986). Although two-dimensional images already reveal much information, a three-dimensional visualization is particularly important since development occurs in three dimensions. Reconstructions of complex anatomical structures in three dimensions are of great importance to fully grasp 3D topography of those components and to properly interpret how the structures physically interact with each other. In this way, the individual bones, cartilage, muscles, etc. can be viewed from different angles, which is necessary to correctly characterize the morphology. For this reason, there is a growing demand for 3D digital images and models. Serial histological sectioning (SHS), dissections or clearing and staining are traditional and destructive approaches to obtain morphological 3D data and information. SHS is a procedure entailing the sectioning of thin slices of a specimen or tissue in a consecutive order. The sample first has to be fixed for the preservation of the structural components, stained and embedded prior to sectioning. The sections are then imaged with an optical

microscope and can subsequently be used for microscopic examination or 3D reconstruction of anatomical structures. A drawback of SHS, however, is that it is time-consuming and relies on a destructive protocol. Moreover, when 3D reconstructions are generated based on those histological sections, manual alignment and segmenting of the sections is required prior to reconstructing.

Recently, several automated and non-destructive imaging techniques have been introduced. Those techniques are able to generate virtual serial sections in any orientation (e.g. frontal, sagittal or transversal) that can be processed digitally to expedite analysis of biological samples. This is the case for X-ray micro Computed Tomography (µCT) scanning (Masschaele et al., 2007; Cnudde et al., 2011), Light Sheet (based) Fluorescence Microscopy (LSFM) (Santi, 2011; Buytaert et al., 2012), Optical Projection Tomography (OPT) (Sharpe et al., 2002), standard and phase-contrast synchrotron X-ray imaging (Betz et al., 2007; Boistel et al., 2011) and magnetic resonance imaging (MRI) (Tyszka et al., 2005; Pohlmann et al., 2007). LSFM uses laser light sheets to illuminate a fluorescent and transparent sample, while OPT uses light rays to image a transparent sample. Synchrotron X-ray imaging uses electromagnetic radiation. MRI uses magnetic fields and radio waves to image the specimen and detects differences in water content and distribution of fluids in the soft tissues near or around bones in a sample. µCT-scanning, which uses X-rays to create cross-sections in a sample, is based on contrast differences in X-ray absorption (i.e. the attenuation contrast between different tissues). All techniques mentioned

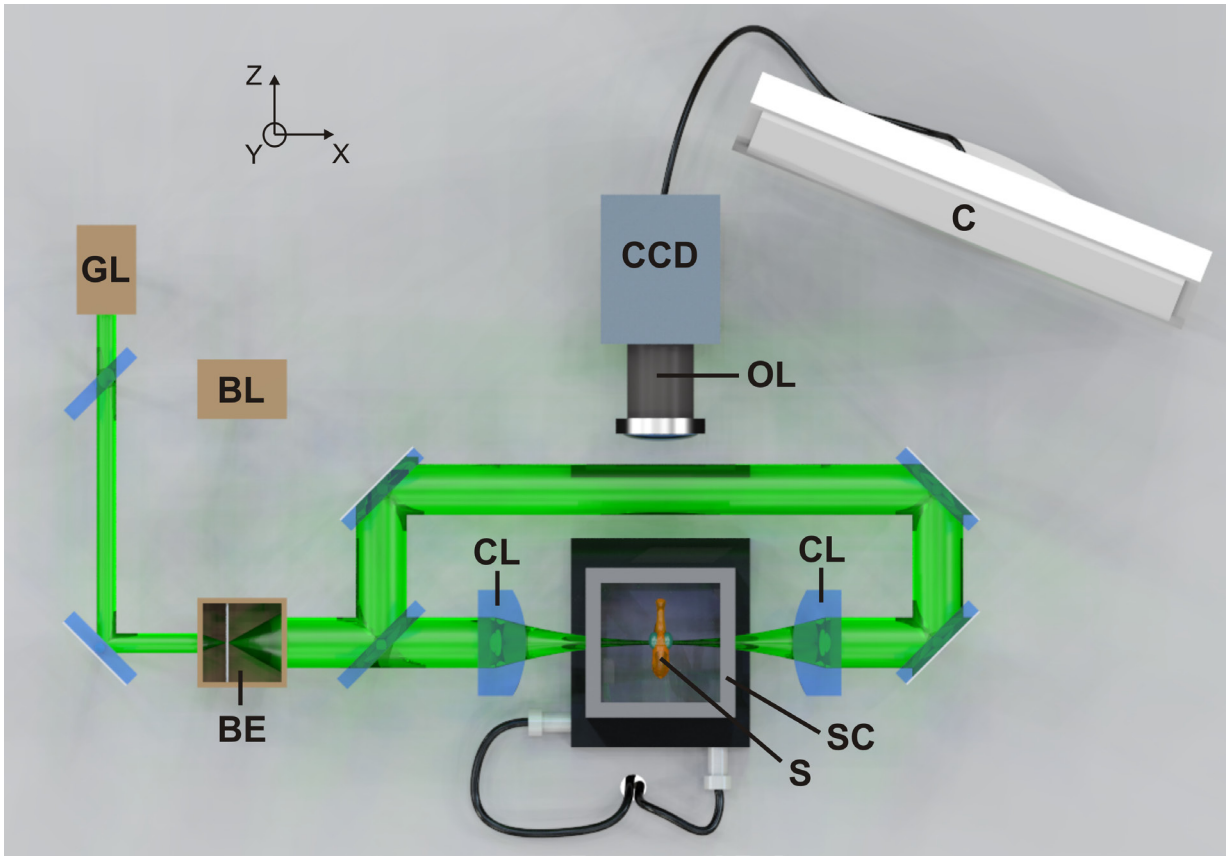

Fig. 1. – Top view of a three-dimensional representation of the (HR)-OPFOS set-up. In this case the green laser (GL) is active, while the blue laser (BL) is not active. The laser light first passes through a beam expander (BE) to increase the diameter of the input beam in the Y and Z dimensions and subsequently passes a cylindrical lens (CL) to focus the beam into a thin light bundle (reducing the beam in the Z-dimension) before it transverses the transparent and fluorescent sample. The sample is immersed in Spalteholz fluid and lies in a sample chamber (SC). The sample emits fluorescent light, which is projected on a CCD camera with an objective lens (OL). The light forms images of the optical sections that are displayed on a computer (C).

above are useful to display the biological specimens in three dimensions, despite the specific limitations of each one. An important constraint of non-destructive approaches is the initial investment in the required infrastructure (e.g. synchrotron facilities). Other techniques suffer from resolution limitations or lack the capability to discriminate between different tissue types, while others fail in penetrating organ systems of interest to a sufficient depth, hence limiting the size range of samples that can be studied.

In 1993, a new alternative microscopic and tomographic approach, the Orthogonal-Plane Fluorescence Optical Sectioning microscopy (OPFOS) emerged in order to simplify the generation of 3D models of complex structures and to make quantitative measurements of the mammalian cochlea (VOIE et al., 1993). OPFOS is a whole-volume imaging method that creates virtual sections by projecting a thin sheet of laser light through the fluorescent and transparent sample (Fig. 1). The sample is excited by the laser light and the fluorescent and autofluorescent light is detected orthogonally with an objective and recorded by a camera. The sample is moved along the Z-axis through the laser light sheet and recorded at different depths. In this way, virtual sections are compiled throughout the specimen and used to generate 3D reconstructions.

OPFOS belongs to a whole new microscopy field, designated Light Sheet based Fluorescence Microscopy (LSFM) (SANTI, 2011; BUYTAERT et al., 2012), including many other implementations such as Selective Plane Illumination Microscopy (SPIM) (HUISKEN et al., 2004), high resolution (HR-) OPFOS (BUYTAERT & DIRCKX, 2007), Ultramicroscopy (DODT et al., 2007) and Thin-Sheet Laser Imaging Microscopy (TSLIM) (SANTI et al., 2009). SPIM has already been used in a study of *in vivo* imaging of the embryogenesis of *Drosophila melanogaster* and muscles in Medaka fishes (HUISKEN et al., 2004). Of the dozens of LSFM implementations, however, only Ultramicroscopy, TSLIM and (HR-)OPFOS (BUYTAERT & DIRCKX, 2007) are capable of imaging macroscopic samples (size range of tens of millimeters). For instance, membranes, suspensory tissues and bones of the middle ear and inner ear were investigated with OPFOS (VOIE, 2002; HOFMAN et al., 2008; BUYTAERT & DIRCKX, 2009; HOFMAN et al., 2009; BUYTAERT et al., 2010; BUYTAERT et al., 2011) and TSLIM (SANTI et al., 2009). Whole mouse embryos and particularly their brains have also been studied with Ultramicroscopy (BECKER et al., 2008). Despite the great utility of LSFM implementations, it has not yet found its way into many fields of biology.

A qualitative comparison between 3D imaging of the musculoskeletal system in a vertebrate head using a completely destructive, largely manual technique (SHS) and a much less destructive, largely digital technique (OPFOS) was conducted in this study. The main purpose of this investigation was to give an overview of the advantages and disadvantages of the use of OPFOS compared to SHS in generating a 3D reconstruction of a similar specimen. In the present study, OPFOS has been applied for the first time on the model organism *Xenopus laevis*. A tadpole of *Xenopus* is a suitable model organism as it is small with a semi-transparent skin that allows a non-invasive investigation of the anatomy of all internal structures. We hypothesized that the 3D models would be more accurate using OPFOS instead of histological sections, since no alignment of the images is necessary and no tissue distortion is induced by mechanical slicing. In addition, shrinking of organs, induced by elaborate specimen preparation, is a well-known phenomenon with both OPFOS (BUYTAERT et al., 2012) and histological sectioning (LANE & RALIS, 1983; HOFMAN et al., 2009). However, we expected that the shrinking effects would be uniform and thus largely negligible for the interpretation of the 3D anatomy.

With the OPFOS method, both omnidirectional fluorescence and autofluorescence can be recorded. Many tissue components exhibit autofluorescence, which is a natural light

emission. The molecules responsible for this spontaneous tissue fluorescence include flavins, nicotinamide adenine dinucleotide (NADH), lipofuscin, elastin, collagen and porphyrins (ANDERSSON et al., 1998; BILLINTON & KNIGHT, 2001). Therefore, we expected to find differences between tissues with distinct autofluorescence values. We also expected that discrimination between different tissue types and organs may be done in an automated way, since different tissue types and organs may display different intensities of autofluorescence. Finally, we wanted to test the potential of this method for discrimination between different structures of the same tissue type (e.g. muscle-muscle or skeleton-skeleton).

MATERIALS AND METHODS

Specimen preparation

Three African clawed tadpoles (*Xenopus laevis*) were used, one in stage 46 for histological sectioning and light microscopy, and two in stage 47 for OPFOS microscopy. This difference in developmental stage is too small to hinder the comparison and should not be considered as an explicative factor for the observed differences. These organisms were macroscopic, which means that they could be perceived by the naked eye, a requirement for the set-up of the OPFOS used in this study. The *Xenopus* larvae were euthanized by MS222 (Sigma E10521) and fixed by immersion in 4% paraformaldehyde. Thereafter, the specimens were processed for dehydration through an ethanol series (30%, 50%, 70% and 100%).

Procedure for SHS

Once placed in 100% ethanol, the specimen was processed for embedding in Technovit 7100 (Heraeus Kulzer Wehrheim, Germany). Serial histological cross-sections of 5µm (slice thickness) were cut using a Leica Polycut SM 2500 microtome. Each section was mounted on a glass slide, stained with toluidine blue and covered. A total of 237 histological sections were used for further investigation. Digital images of those sections were taken using a Colorview8 CCD camera (SIS) placed on a Reichert Polyvar microscope, managed by the software program analySIS 5.0. The pictures of the sections were loaded in the 3D graphics software Amira 5.0 - Visage Imaging (64-version, Mercury Computer Systems) and aligned semi-automatically. Different anatomical structures were identified, but only relevant structures (i.e. muscles and cartilaginous elements of the cranium) were segmented (isolated digitally) manually. A virtual 3D-reconstruction was then generated based on those segmented structures.

Procedure for OPFOS

The OPFOS technique required an elaborate specimen preparation (VOIE, 2002; BUYTAERT & DIRCKX, 2009). Between the fixation step and the dehydration step, the tadpoles needed to be bleached. Tadpoles have a pigmented skin, hence, they were bleached in a 5% hydrogen peroxide solution (H_2O_2) for one hour. After that, they were cleared and optionally stained with a fluorescent dye. The clearing process involved placing the specimens in a graded series of Spalteholz fluid (25%, 50%, 75%, 100% and 100%), which consists of five volumes of methylsalicylate (oil of wintergreen) and three volumes of benzyl benzoate. This method matches the refraction index of the entire sample to that of the fluid, making the entire sample optically transparent. In this study, a blue laser light was used for the illumination of the sample. The sample emitted autofluorescence at a wavelength of 488 nm.

With OPFOS, a FOculus FO531SB grayscale camera (NET GmbH) was used, equipped with a combined QIOPTIC Optem Zoom 125C optical lens system comprising a 1x Qioptiq art 30-13-10 (15 mm fine focus module), a 1x Qioptiq art 30-61-40 (zoom module with detents, no iris) and a 1x Qioptiq art 29-90-73 (1.5x TV tube). Pictures with pixelsize 2.3 x 2.3 µm were taken of the illuminated plane every 3µm and stored. The collected image data had a bit-depth of 12-bit (4096 gray-scale values). Up to 567 images

were loaded in the 3D graphics software program Amira 5.0 - Visage Imaging (64-bit version, Computer Systems Mercury). For comparison, the anatomical structures labeled for SHS were identified and segmented manually based on gray-scale values. 3D reconstructions of the labeled structures were then generated.

Advantages and disadvantages of shs

The SHS technique provides high resolution images (the only limitation is the resolution of the optics of the light microscope) and results in detailed 3D reconstructions. The major structures can be discerned down to the cellular level, where individual cells can be seen clearly. Sometimes, even details down to the subcellular level can be identified. The high quality imagery is highlighted in Figure 2 (A-B). One of the advantages of SHS is that the sections are always accessible. Later, it is possible to go back to the samples and look for specific details. Tissue types such as muscle tissue, skeletal tissue and neural tissue can be discerned very easily based on the staining of the sections (Figs 2 and 3). In this study, the muscles as well as the structures of the nervous system are stained entirely, resulting in blue structures of variable blue gradients discernible from each other. On the contrary, the cartilaginous skeletal structures are not stained completely, as only the extracellular matrix, the chondrocytes and nuclei are stained blue (Fig. 3C). The lacunae, being occupied by the chondrocytes (which are unfortunately not well preserved during fixation), are large cavities in the matrix, appearing white after the sections have been stained. With the light microscopic histology technique, bones as well as cartilage can be visualized simultaneously. Since the animals in our study were too young, bone was not present, but the technique would allow visualization of cartilage and bone.

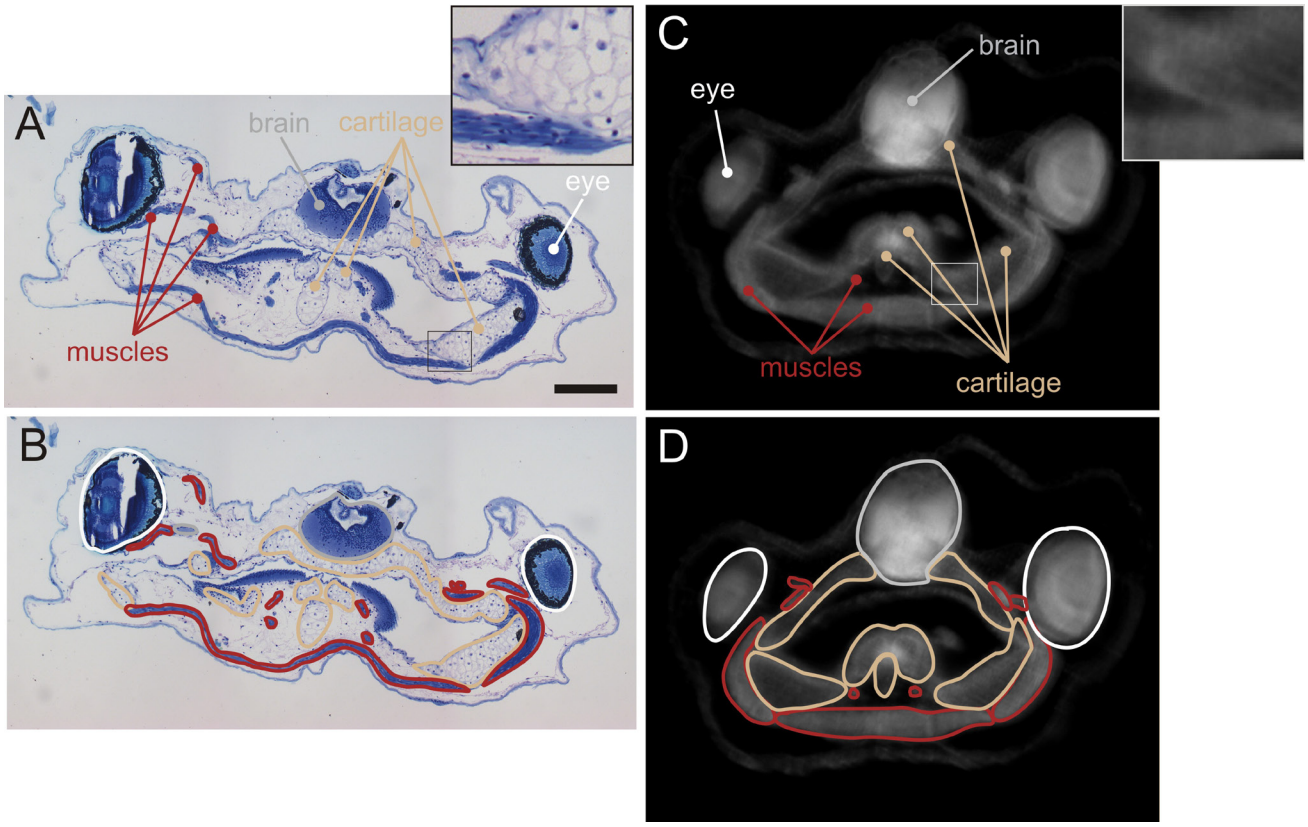

Fig. 2. – Cross-sections of the head of *Xenopus laevis* tadpoles generated with (A,B) histological sectioning and (C,D) OPFOS. The colored lines on panels (B,D) demonstrate the labeling of the different structures before 3D reconstruction. Magnification of some cartilage and muscle tissues is shown in the upper right insets of panels (A,C). Scale bar: 200 µm.

The SHS technique is, however, labour-intensive and particularly time-consuming. First, the specimens need to be fixed, decalcified (when they contain mineralized bone) and dehydrated. After this, the specimens have to be sectioned mechanically (one cutting direction) in very thin slices, and are thus destroyed. For this reason, the sample cannot be used more than once or used for other purposes. Next, pictures of the sections have to be taken and saved individually. Consequently, image processing and registration are necessary and quite difficult. Accordingly, not every section is included in a traditional reconstruction, because this would increase the workload to take pictures of every slice at a high resolution. This also means that every virtual section that diverges in orientation from the cutting plane (i.e. along the Z-axis) will provide fewer details. Thereafter, the spatial alignment of the slices into a 3D dataset has to be done manually and artefacts can be introduced through imperfect aligning. The latter are partially induced by mechanical deformation of the sections as a result of sectioning and subsequent stretching (Fig. 3 A-B), and partially because there are often no adequate reference points for the alignment of the sections. Because of misalignment and distortion in individual slices, the final 3D reconstruction is less smooth, giving it an impression of having a rough surface (Fig. 4). The position of the individual sections can still be seen on the 3D reconstruction, which can be due to manual alignment, deformation caused by cutting the sample, and the smaller number

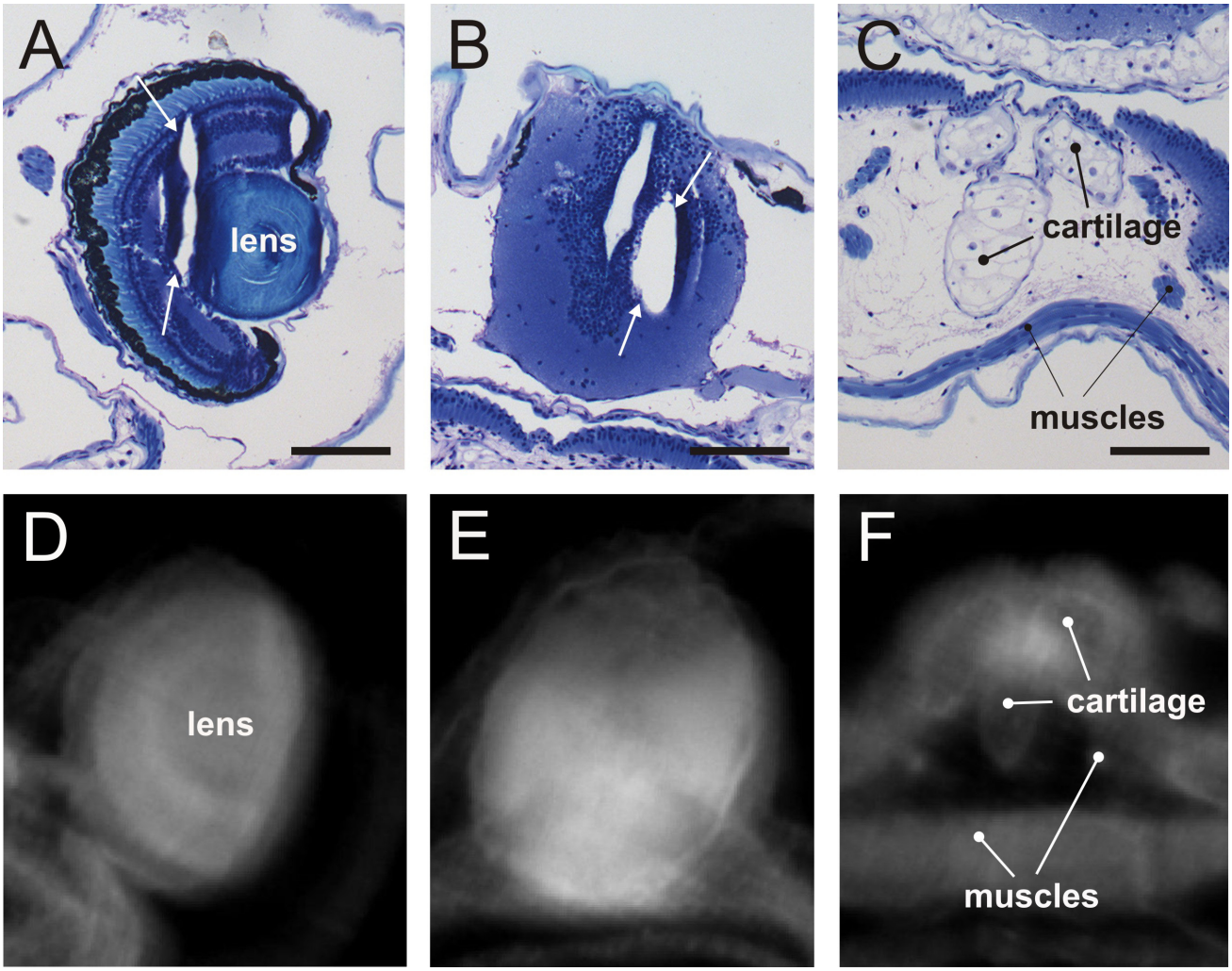

Fig. 3. – Comparison between the two techniques: (A-C) histological sectioning and (D-F) OPFOS. Cross-sections at the level of (A,D) eye; (B,E) brain; (C,F) cartilage and muscles. Arrows show artifacts in the histological sections due to specimen preparation. Scale bar: 100 µm.

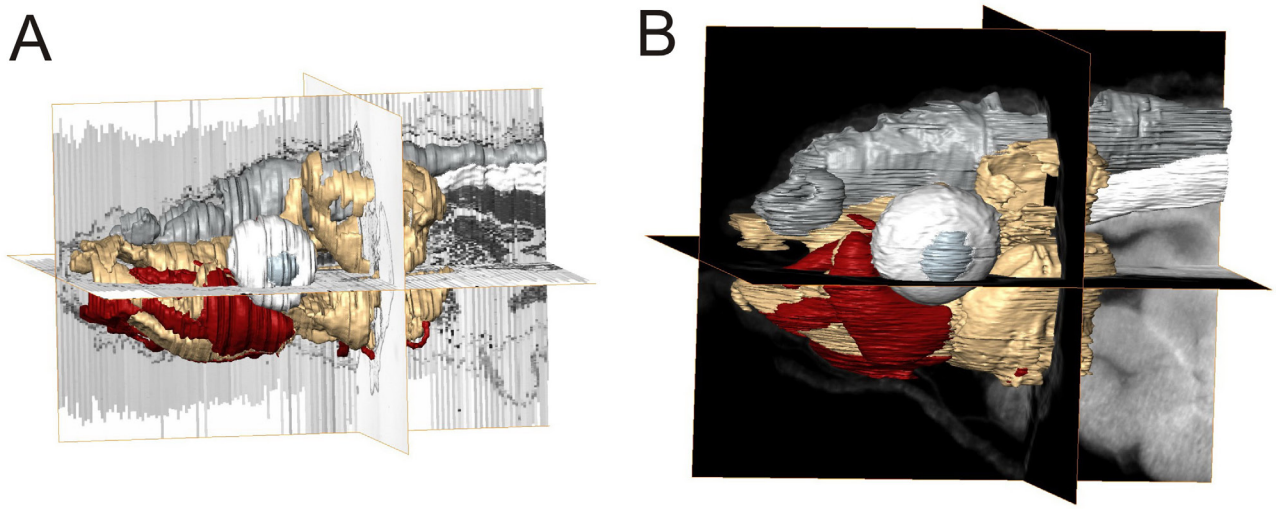

Fig. 4. – Lateral view of two 3D reconstructions of *Xenopus laevis* head with cross sections in three orientations generated with (A) histological sectioning and (B) OPFOS. Different colors represent different tissue types (beige: cartilage, red: muscles, grey: brain and nervous system).

of sections used for the reconstruction (as only a fraction of all available sections is used). In the latter case, the distance between two successive sections is larger than the X- and Y-voxel size. Moreover, artefacts such as shape distortions of tissues are unavoidable. In this study, for example, the reconstructed specimen seems to be dorsoventrally flattened and especially the brain appears to be collapsed (Fig. 4). This kind of distortion, which may be due to mechanical slicing (knife orientation), cannot be undone. Some distortions can sometimes be partially undone by supplementary manual adaptations, such as interpolating the tissue segmentations on the sections just before and just after the distorted section. Finally, light microscopic histology, as applied in this study, relied on the use of expensive instruments including a microtome, a

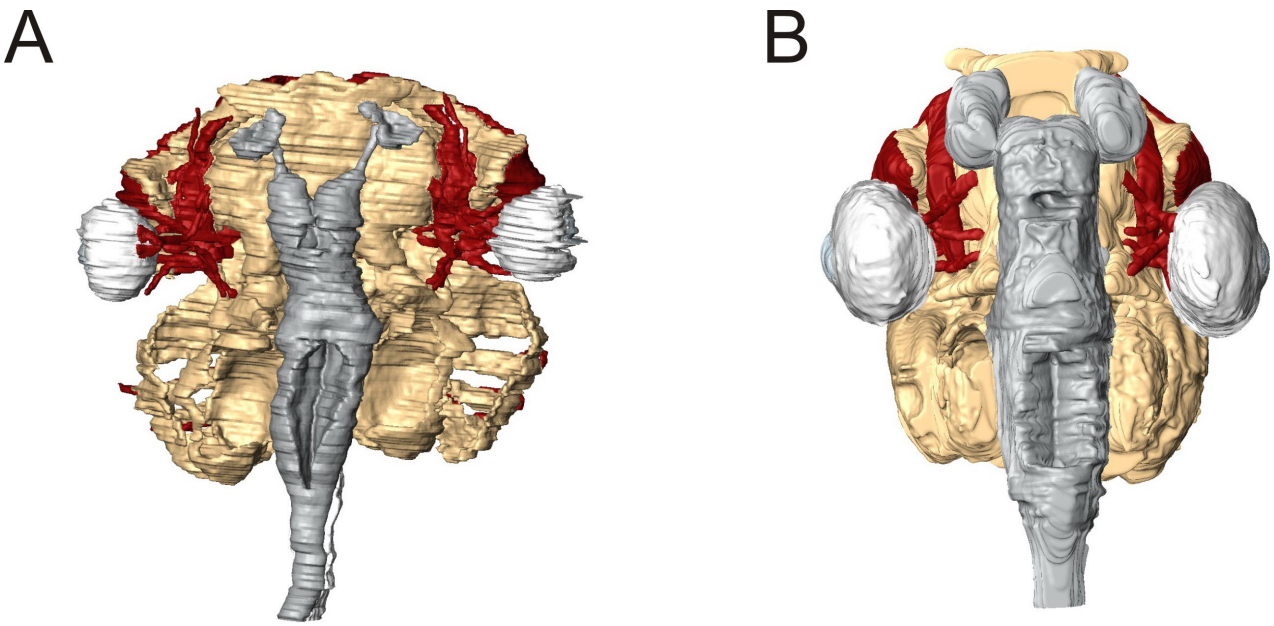

Fig. 5. – Dorsal side of 3D models of *Xenopus laevis* heads, using (A) histological sectioning and (B) OPFOS.

histokinette, an automatic glass coverslipper, a stereomicroscope and a camera.

Advantages and disadvantages of opfos

The virtual sectioning and imaging are performed quickly and in real-time, and are consequently less time-consuming. There are no registration difficulties as image registration between successive sections is done automatically. The data do not need to be aligned, since it is a whole-mount and semi-destructive imaging technique, where the data are already aligned in the image database. This advantage leads to a smooth 3D reconstruction. Moreover, the images obtained with the OPFOS technique have a good resolution. The highest axial resolution (Z-dimension) that can be obtained with high resolution (HR-)OPFOS is 2µm (Buytaert & Dirckx, 2007). Lateral (X and Y) dimensions can even go below micron level. In the sections in this study, an axial resolution of about 5 µm was obtained. Region-of-interest imaging, which is the imaging of only a substructure of the object, can be performed with OPFOS. This may deliver detailed microscopic and even histological information (at cellular level). However, since ours are preliminary data, no region-of-interest has been imaged. This approach is suited to visualization of bony structures (after decalcification) and soft tissues (such as muscles and nerves) at the same time. The different tissue types, such as muscle tissue and skeletal elements, can be discriminated very easily by their own tissue-specific gray levels. The obtained images are thus composed of different grayscales (Figs 2 and 3). Skeletal structures are darkest on the OPFOS images, reflecting the lowest levels of autofluorescence while the muscles and nervous system are the brightest structures. The boundary between two adjacent structures, having different tissue types, can be discerned based on those distinct grayscales and their mutual topography. This allows manual tracing (Fig. 2D) and the generation of a 3D reconstruction (Figs 4B and 5B) of the individual structures on the image stacks acquired by OPFOS. If two adjacent structures have the same tissue type (e.g. muscle-muscle) and thus the same gray levels, however, prudence and knowledge on the anatomy are called for in the interpretation of their boundary depending on the quality of the images.

OPFOS microscopy is a whole-volume imaging method that does not destruct or touch the specimen, since a laser light sheet is used to generate the sections. Therefore, several 2D images series can be recorded with a different slicing orientation and one specimen can be used multiple times. Moreover, all structures remain in their natural position and there are no artefacts due to an imperfect alignment of the optical sections. Furthermore, functional staining with a fluorescent dye (such as Rhodamine B) can be applied in order to obtain stronger fluorescence and to better discriminate between tissue types. Even multiple dyes can be incorporated to stain different tissue types, though each requires its own specific laser light source that emits light of a specific wavelength. Another advantage of OPFOS microscopy in this study is that it utilised relatively inexpensive components, including a sample chamber, a light source, a CCD camera and optics. This makes the OPFOS accessible to a larger group of researchers.

The preparation of the specimen is, however, extensive (Voie, 2002; Buytaert & Dirckx, 2009). An elaborate procedure must be followed: fixation, bleaching, EDTA decalcification, dehydratation and refractive index matching or clearing. The bleaching with hydrogen peroxide and decalcification with EDTA are optional and irreversible, although they are required when pigmented tissue and calcium content are present. In the first specimen that was scanned with OPFOS, the light was blocked or attenuated in some parts of the sample due to remaining pigmentation. Consequently, the OPFOS images were reduced in quality as typical striped shadows (black masses) (Buytaert & Dirckx, 2009; Buytaert et al., 2011; Buytaert et al., 2012) were generated in the images (Fig. 6). This is caused when the illumination sheet originates from only one side of the image. When the laser

sheet then encounters a pigment, the light and thus also the tissues behind this pigment are attenuated, resulting in shadow artifacts. Those black masses make it difficult to segment the missing structures prior to 3D reconstructing. To solve that problem, the method was refined during the experiment by adding an additional bleaching step. Two-sided illumination (Fig. 1) partially solves this problem too. However, this requires a more difficult calibration and aligning of the set-up. In this study, the two-sided illumination unfortunately resulted in blurred images (Figs 2 and 3). Sharper images would reduce the time of segmentation of each structure and even allow this segmentation in a semi-automated or automated way. Such sharper images may be obtained by a thinner laser light plane, a lens objective of a better quality, less vibrations and a higher resolution of the camera.

Fig. 6. – Virtual section of the head of a *Xenopus laevis* tadpole generated with OPFOS. At the level of the arrows, where a structure is expected, a black region is noticed. This is due to pigmentation on the tadpole's skin, resulting in blocked or attenuated light.

Other steps in the preparation process are decalcification and clearing. Calcium, which is the main component of bone, scatters light strongly. In this study, the specimens had no bony structures, so no decalcification was necessary. Clearing of specimens leads to their irreversible transparency, preventing, for example, any histological post-processing. After specimen preparation and imaging, anatomical structures on hundreds of sections have to be segmented manually – a time-consuming procedure.

Summary of similarities and differences in methods

Both OPFOS and SHS techniques required elaborate specimen preparation. Refractive index matching and bleaching were extra steps in the preparation process of OPFOS over histology. The OPFOS set-up was very sensitive to remaining eye and skin pigmentation, necessitating bleaching of the tadpole in order to make pigmented tissue transparent. Interestingly, the bleaching step is not necessary for specimens that become sufficiently transparent during the specimen preparation (e.g. young seahorses). Moreover, the real-time virtual sectioning of OPFOS makes it an ideal tool for fast screening of macroscopic animals (size range of tens of millimeters), while SHS requires manual, labour-intensive and destructive sectioning. As the OPFOS technique is semi-destructive, the specimens can, however, not be used again for histological sectioning or immunohistochemical analysis afterwards. This is actually possible with samples scanned with, for example, µCT. OPFOS-like techniques nevertheless suffer from the fact that the specimens are made irreversibly transparent. This is also the case with OPT (Optical Projection Tomography), but not with µCT and MRI, where the specimens can be reused for other purposes. An advantage of OPFOS over OPT and µCT is that the cross sectional area is immediately registered, while with OPT and µCT the data first needs back-

projection calculations to recreate the original object (Kak & Slaney, 1988).

2D sections with microscopic details were generated with SHS, while with OFPOS fewer details were revealed. Even in 3D, SHS showed more details than OPFOS. Particular structures can be visualized with SHS using a staining protocol comprising several dyes. Some staining protocols are capable of staining cellular structures, such as myelin, muscle striations, etc. In the same way, functional staining has the potential to be applied to OPFOS.

OPFOS does have the simplicity of allowing discrimination between tissue types of different organ systems thanks to their distinctly different grayscales because it relies on (native) tissue contrast. On the other hand, SHS depends on histological staining, where as a result even the same tissue might have a different color intensity from section to section. On the virtual sections of OPFOS, differences between tissues with distinct autofluorescence values were found as expected. However, a problem arises using OPFOS where organ systems having similar tissue types lie side by side (i.e. muscle-muscle) and have similar grayscale values. The combination of blurred images and similar tissue types resulted in images that were of insufficient quality to generate an accurate 3D model. In this case, the boundary between different structures could not always be accurately determined. This limitation prevented automatic discrimination of different tissue types. The histological sections were therefore very useful for labeling the virtual sections of OPFOS.

One of the biggest advantages of both OPFOS and SHS is their ability to visualize bony structures and soft tissues simultaneously. This is also an advantage for MRI (Tyszka et al., 2005; Pohlmann et al., 2007) and OPT. Using simple staining techniques, including contrast agents such as osmium tetroxide (OsO_4) or phosphotungstic acid (PTA), µCT can provide high-contrast 3D imaging of soft tissues as well (Johnson et al., 2006; Metscher, 2009a, b).

The 3D reconstructions showed that the OPFOS provided a more naturally-shaped 3D model than the one based on histological sections. With OPFOS, all structures remained in their natural position, while in the reconstructions generated with histological sections small irregularities as well as an apparent flattening of the 3D model were discernible (Fig. 4). Using SHS, all sections needed to be aligned manually, which in practice could not be done without artefacts. Extra compensations were also necessary for distortions due to the preparation procedure of the sections. Another kind of distortion, which occurred in both SHS and OPFOS, is shrinking. Shrinking of tissues in all three dimensions was previously reported for OPFOS (Voie, 2002; Hofman et al., 2008; Buytaert et al., 2011). This shrinking is induced by the elaborate specimen preparation (fixation, decalcification and dehydration). On the other hand, shrinking is also well-known to occur in SHS as the preparation also includes fixation, (decalcification) and dehydration (Lane & Ralis, 1983). Therefore, deformations due to specimen preparation were expected with both protocols. Comparing both 3D reconstructions, we noticed that our OPFOS model looked different from the SHS model as if some structures have shrunk in the SHS model (Fig. 5). Most obvious were the smaller eyes and nasal capsules, indicating a more invasive influence of the SHS procedure on the specimen. In this way, our hypothesis that a more accurate 3D model is obtained with the OPFOS technique can thus be confirmed.

The highest resolution for macroscopic specimens, which is about 0.2µm, is provided by standard histological sections. In our study, the 2D histological sections provided a better resolution than OPFOS. The attainable resolution with (HR-)OPFOS is around 2µm for macroscopic specimens (Buytaert & Dirckx, 2007), but in this study it was 5µm. It is, however, to be expected that SHS will always slightly outperform OPFOS on resolution of 2D section images. Other LSFM methods, however, can achieve submicron resolution on microscopic samples. Regarding other modern automated techniques, µCT can

currently easily reach a resolution of 1µm (MASSCHAELE et al., 2007) and sometimes even resolutions of 700nm (CNUDDE et al., 2011). Real-time synchrotron X-ray phase-contrast imaging (SOCHA et al., 2007) is capable of reaching a resolution of about 1µm, but there is an important trade-off between the spatial resolution and the detrimental effects on the specimen. OPFOS has conversely a higher resolution than OPT (Optical Projection Tomography), which is limited to a resolution of 5 to 10µm (SHARPE et al., 2002), and MRI, which attains a lower resolution of about 25µm (SCHNEIDER et al., 2003b, c; SCHNEIDER et al., 2003a).

Finally, the infrastructure cost for the basic implementation of OPFOS microscopy used in this study was estimated to be more than 15 times lower than that for SHS. Newer and better OPFOS devices are still cheaper than SHS. Other expensive imaging techniques are for example the µCT scanning, MRI and synchrotron X-ray imaging (SANTI, 2011).

FUTURE ADVANCES AND CONCLUSIONS

From our preliminary study, we can conclude that OPFOS tomography is a good technique for the investigation of musculoskeletal systems in macroscopic specimens, as shown here for tadpoles. As expected, SHS achieved a better spatial resolution, which is important to see microscopic details and obtain essential information. Unfortunately, this could not be obtained with the basic implementation of the OPFOS technique used in this study. Several improvements to the (HR-)OPFOS tomography have already been made (BUYTAERT et al., 2011) and the LSFM field is still evolving. Therefore, a more elaborate comparison that includes more advanced OPFOS versions would be useful to get a better overview of the advantages and disadvantages.

ACKNOWLEDGEMENTS

This work was supported by the Concerted Research Actions (GOA - 01G01908) of Ghent University, and by the Research Foundation - Flanders.

REFERENCES

AFSHAR F & DYKES E (1982). A three-dimensional reconstruction of the human brain stem. Journal of Neurosurgery, 57: 491-495.

ANDERSSON H, BAECHI T, HOECHL M & RICHTER C (1998). Autofluorescence of living cells. Journal of Microscopy, 191: 1-7.

BECKER K, JAEHRLING N, KRAMER ER, SCHNORRER E & DODT HU (2008). Ultramicroscopy: 3D reconstruction of large microscopical specimens. Journal of Biophotonics, 1: 36-42.

BETZ O, WEGST U, WEIDE D, HEETHOFF M, HELFEN L, LEE WAHK & CLOETENS P (2007). Imaging applications of synchrotron X-ray phase-contrast microtomography in biological morphology and biomaterials science. I. General aspects of the technique and its advantages in the analysis of millimetre sized arthropod structure. Journal of Microscopy, 227: 51-71.

BILLINTON N & KNIGHT AW (2001). Seeing the wood through the trees: a review of techniques for distinguishing green fluorescent protein from endogenous autofluorescence. Analytical biochemistry, 291: 175.

BOISTEL R, SWOGER J, KRŽIČ U, FERNANDEZ V, GILLET B & REYNAUD EG (2011). The future of three-dimensional microscopic imaging in marine biology. Marine Ecology, 32: 438-452.

BUYTAERT JAN & DIRCKX JJJ (2007). Design and quantitative resolution measurements of an optical virtual sectioning three-dimensional imaging technique for biomedical specimens, featuring two-micrometer slicing resolution. Journal of Biomedical Optics, 12: 0140391.

BUYTAERT JAN & DIRCKX JJJ (2009). Tomographic imaging of macroscopic biomedical objects in high resolution and three dimensions using orthogonal-plane fluorescence optical sectioning. Applied Optics, 48: 941-948.

BUYTAERT JAN, DESCAMPS E, ADRIAENS D & DIRCKX JJJ (2010). Orthogonal-Plane

Fluorescence Optical Sectioning: a technique for 3-D imaging of biomedical specimens. *In*: Mendez-Vilas A. & Díaz J., editors. Microscopy: Science, technology, applications and education. Formatex Research Center. pp. 1356-1365.

Buytaert JAN, Descamps E, Adriaens D & Dirckx JJJ (2012). The OPFOS microscopy family: high-resolution optical-sectioning of biomedical specimens. Anatomy Research International, 2012: 9 pages.

Buytaert JAN, Salih WHM, Dierick M, Jacobs P & Dirckx JJJ (2011). Realistic 3D Computer Model of the Gerbil Middle Ear, Featuring Accurate Morphology of Bone and Soft Tissue Structures. Journal of the Association for Research in Otolaryngology, 12: 681-696.

Cnudde V, Boone M, Dewanckele J, Dierick M, Van Hoorebeke L & Jacobs P (2011). 3D characterization of sandstone by means of X-ray computed tomography. Geosphere, 7: 54-61.

Dodt H-U, Leischner U, Schierloh A, Jaehrling N, Mauch CP, Deininger K, Deussing JM, Eder M, Zieglgaensberger W & Becker K (2007). Ultramicroscopy: three-dimensional visualization of neuronal networks in the whole mouse brain. Nature Methods, 4: 331-336.

Hofman R, Segenhout JM & Wit HP (2009). Three-dimensional reconstruction of the guinea pig inner ear, comparison of OPFOS and light microscopy, applications of 3D reconstruction. Journal of Microscopy, 233: 251-257.

Hofman R, Segenhout JM, Buytaert JAN, Dirckx JJJ & Wit HP (2008). Morphology and function of Bast's valve: additional insight in its functioning using 3D-reconstruction. European Archives of Oto-Rhino-Laryngology, 265: 153-157.

Huisken J, Swoger J, Del Bene F, Wittbrodt J & Stelzer EHK (2004). Optical sectioning deep inside live embryos by selective plane illumination microscopy. Science, 305: 1007-1009.

Johnson EM & Capowski JJ (1983). A system for the three-dimensional reconstruction of biological structures. Computers and Biomedical Research, 16: 79-87.

Johnson JT, Hansen MS, Wu I, Healy LJ, Johnson CR, Jones GM, Capecchi MR & Keller C (2006). Virtual histology of transgenic mouse embryos for high-throughput phenotyping. Plos Genetics, 2: 471-477.

Kak A & Slaney M (1988). Principles of computerized tomographic imaging. IEEE Press, New York, 329 pp.

Lane J & Ralis ZA (1983). Changes in dimensions of large cancellous bone specimens during histological preparation as measured on slabs from human femoral heads. Calcified Tissue International, 35: 1-4.

Masschaele BC, Cnudde V, Dierick M, Jacobs P, Van Hoorebeke L & Vlassenbroeck J (2007). UGCT: New X-ray radiography and tomography facility. Nuclear Instruments and Methods in Physics Research Section A: Accelerators, Spectrometers, Detectors and Associated Equipment, 580: 266-269.

Metscher BD (2009a). MicroCT for comparative morphology: simple staining methods allow high-contrast 3D imaging of diverse non-mineralized animal tissues. BMC Physiology, 9: 11.

Metscher BD (2009b). MicroCT for developmental biology: A versatile tool for high-contrast 3D imaging at histological resolutions. Developmental Dynamics, 238: 632-640.

Pohlmann A, Möller M, Decker H & Schreiber WG (2007). MRI of tarantulas: morphological and perfusion imaging. Magnetic Resonance Imaging, 25: 129-135.

Santi PA (2011). Light Sheet Fluorescence Microscopy: A Review. Journal of Histochemistry & Cytochemistry, 59: 129-138.

Santi PA, Johnson SB, Hillenbrand M, GrandPre PZ, Glass TJ & Leger JR (2009). Thin-sheet laser imaging microscopy for optical sectioning of thick tissues. Biotechniques, 46: 287-294.

Schneider JE, Bamforth SD, Grieve SM, Clarke K, Bhattacharya S & Neubauer S (2003a). High-resolution, high-throughput magnetic paragraph sign resonance imaging of mouse embryonic paragraph sign anatomy using a fast gradient-echo sequence. Magma 16: 43-51.

Schneider JE, Bamforth SD, Farthing CR, Clarke K, Neubauer S & Bhattacharya S (2003b). High-resolution imaging of normal anatomy, and neural and adrenal malformations in mouse embryos using magnetic resonance microscopy. Journal of Anatomy, 202: 239-247.

Schneider JE, Bamforth SD, Farthing CR, Clarke K, Neubauer S & Bhattacharya S (2003c). Rapid identification and 3D

reconstruction of complex cardiac malformations in transgenic mouse embryos using fast gradient echo sequence magnetic resonance imaging. Journal of Molecular and Cellular Cardiology, 35: 217-222.

Sharpe J, Ahlgren U, Perry P, Hill B, Ross A, Hecksher-Sorensen J, Baldock R & Davidson D (2002). Optical projection tomography as a tool for 3D microscopy and gene expression studies. Science, 296: 541-545.

Socha J, Westneat M, Harrison J, Waters J & Lee WK (2007). Real-time phase-contrast x-ray imaging: a new technique for the study of animal form and function. BMC Biology, 5: 6.

Tyszka JM, Fraser SE & Jacobs RE (2005). Magnetic resonance microscopy: recent advances and applications. Current Opinion in Biotechnology, 16: 93-99.

Vanden Berghe WV, Aerts P, Claeys H & Verraes W (1986). A microcomputer-based graphical reconstruction technique for serial sectioned objects, with hidden line removal. The Anatomical Record, 215: 84-91.

Voie AH (2002). Imaging the intact guinea pig tympanic bulla by orthogonal-plane fluorescence optical sectioning microscopy. Hearing Research, 171: 119-128.

Voie AH, Burns DH & Spelman FA (1993). Orthogonal-plane fluorescence optical sectioning - 3-Dimensional imaging of macroscopic biological specimens. Journal of Microscopy-Oxford, 170: 229-236.

Received: November 11th, 2011

Accepted: January 20th, 2012

Branch editor: Vanhooydonck Bieke